Journal of Power Sources 655 (2025) 237905

Contents lists available at ScienceDirect

Journal of Power Sources

journal homepage: www.elsevier.com/locate/jpowsour

Adsorption thermodynamics of methane reforming over solid oxide fuel cell anodes

Saeed Moarrefi [a], Mohammad Rajabi Naraki [b], Mohan Jacob [a], Nilay Shah [c], Stephen Skinner [d], Lichao Jia [e], Shou-Han Zhou [f], Weiwei Cai [g], Liyuan Fan [h,*]

[a] College of Science and Engineering, James Cook University, 1 James Cook Drive, Townsville, QLD, 4811, Australia
[b] Department of Environment, Land and Infrastructure Engineering, Polytechnic University of Turin, Corso Duca degli Abruzzi, 24, 10129, Torino To, Italy
[c] Department of Chemical Engineering, Imperial College London, London, UK
[d] Department of Materials, Imperial College London, London, UK
[e] School of Materials Science and Engineering, State Key Lab of Materials Processing and Die & Mould Technology, Huazhong University of Science and Technology, Wuhan, 430074, China
[f] Department of Mechanical Engineering, Cardiff University, UK
[g] Faculty of Metallurgical and Energy Engineering, Kunming University of Science and Technology, Kunming, 650093, China
[h] School of Chemistry and Chemical Engineering, Queen's University Belfast, UK

HIGHLIGHTS

- Current density affects Gibbs free energy of CO_2 and H_2O adsorption.
- H_2O shows lower ΔG° values than CO_2, indicating a higher adsorption activity.
- Current density impacts CO_2 and H_2O adsorption differently in fuel cells.
- Adsorption equilibrium constant ratios help optimize anode performance.
- 3D plots show distinct regions for CO_2 and H_2O adsorption spontaneity.

GRAPHICAL ABSTRACT

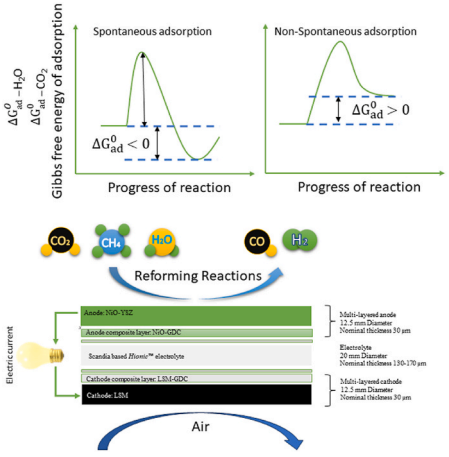

ARTICLE INFO

Keywords:
SOFC
Methane reforming kinetics
Gibbs free energy of adsorption
Langmuir–hinshelwood

ABSTRACT

Adsorption kinetics and thermodynamics on nickel base anode materials remain underexplored under reforming conditions when fuelled directly with methane. The kinetics determine how quickly and effectively reactant gases interact on the anode surfaces, affecting the behavior of subsequent electrochemical reactions. However, the complexity of these interactions under operating conditions have led to a limited number of detailed studies in this area. Thus, further investigation into adsorption kinetics could unlock new possibilities for optimizing fuel

* Corresponding author. School of Chemistry and Chemical Engineering, Queen's University Belfast, UK
E-mail address: l.fan@qub.ac.uk (L. Fan).

https://doi.org/10.1016/j.jpowsour.2025.237905
Received 8 May 2025; Received in revised form 26 June 2025; Accepted 13 July 2025
Available online 23 July 2025

cell performance. This study examines the adsorption Gibbs free energy of reactants on the anode in solid oxide fuel cell to assess the electrocatalyst activity. Our findings reveal that H_2O exhibits more favorable adsorption conditions than CO_2 on the catalyst surface, and increased temperature and current density lead to different surface adsorption behaviours. The results show that steam reforming prevents coke formation on the fuel cell anode more effectively than dry reforming. This proposed method can also be used to examine the coke resistance and the performance of anode structures during the investigation and development stages for fuel cell research. The study provides valuable insights into anode performance and offers a foundation for future advancements in SOFC technology.

1. Introduction

Electrochemical devices provide promising solutions for clean, cost-effective, and sustainable energy production [1]. They balance carbon emissions by utilizing greenhouse gases in electrochemical reactions to mitigate global warming and climate changes [2,3]. The conversion of methane and carbon dioxide from catalytic electrochemical reactions into electricity in solid oxide fuel cells (SOFCs) presents an appealing opportunity to produce carbon-neutral electricity [4–6]. Steam reforming of methane (SRM) is the conventional approach integrated with SOFC systems, involving the reaction of methane (CH_4) with steam (H_2O) to produce syngas containing hydrogen (H_2) and carbon monoxide (CO) [7]. Dry reforming of methane (DRM), uses carbon dioxide (CO_2) instead of steam in this process, offering a more environmentally friendly approach with the potential for higher performance than SRM [8,9]. The widespread adoption of internal methane reforming over SOFCs is hindered by challenges such as carbon deposition, and high material costs, and the lack of understanding of reaction kinetics, and thermochemical equilibrium [10].

One promising approach to address the abovementioned challenges involves using cost-effective materials, such as nickel base ceramic, which demonstrate acceptable durability against impurities and extreme process conditions as anode structures for SOFCs [11,12]. It is widely accepted that the adsorption isotherm in a SOFC is a linear temperature-dependent function. Recent studies reveal that current density also influences this dependency, creating complex electrochemical behaviour over anode functional layers [4,7,9,13]. Extensive efforts have been directed towards developing a consistent methodology to explain various unresolved experimental questions about nickel base ceramic anodes, mainly focusing on their electrocatalytic behavior, which helps researchers to develop more efficient catalysts for SOFC applications. To address the gaps in this emerging field, Thattai et al. [14] investigated the kinetics of internal SRM within nickel base ceramic anodes in an SOFC to develop a model that describes the influence of electrochemical reactions on kinetic parameters.

The reaction mechanism of DRM and SRM has been studied extensively, but there is still ongoing debate about which kinetic models best represent the process inside SOFCs, especially under real operating conditions. Different models have been proposed depending on the catalyst used and the reaction environment. These include the Power-Law (PL), Eley-Rideal (ER), Langmuir-Hinshelwood (LH), and Langmuir-Hinshelwood–Hougen-Watson (LHHW) models [10,14,15]. The PL model is simple and often used to estimate reaction orders, but it does not consider the detailed steps that happen on the catalyst surface [16]. The ER model involves reactions between gas-phase molecules and those adsorbed on the surface [17]. The LH model, used in this study, assumes both reactants first adsorb on the surface before reacting, and it has been widely supported by experimental data [4,9,18]. The LHHW model is able to relate surface reactions to gas-phase concentrations [19,20]. The LH model was selected in this study because it effectively represents surface reactions involving the dissociative adsorption of both CH_4 and CO_2 on the Ni-based anode, aligns well with reported SOFC experimental data, and offers a practical balance between mechanistic relevance and model simplicity for fitting kinetic parameters. While many researchers select the LH model for its simplicity and reasonable accuracy, we acknowledge its limitations, particularly the assumption of ideal adsorption without interactions between surface species, highlighting the limitations of current models [17] and the need for further research on anode materials under current influence. Fan et al. [7] modified previous SRM models and found that current density positively affects the reaction rate, while steam partial pressure negatively impacts it. Their subsequent studies [8,21] revealed that the effect of current density on the steam adsorption constant varies, emphasizing the need for more detailed experimental data across a broader range of temperatures and current densities to improve the proposed kinetic models. Zhou et al. [13] extended Fan et al.'s [7] work by investigating the adsorption kinetics of anodes, providing detailed descriptions of adsorption equilibrium constants, enthalpy, entropy changes, and activation energy concerning current density in the SRM process. Although recent studies offer valuable kinetic parameters for SRM-SOFC, data for DRM-SOFC systems remain sparse. To address this gap, the authors of this study investigated the effects of temperature, gas composition, and current density on the kinetic parameters of DRM in nickel base ceramic anodes [4]. We found that CH_4 partial pressure influences the DRM reaction rate significantly more than CO_2, especially at higher temperatures. Increased current density enhances CO_2 adsorption equilibrium constants and methane conversion.

Most studies have examined DRM and SRM processes on different anode materials, we also conducted a comparative study using the same anode material for DRM and SRM coupled with SOFC. This allowed for a comprehensive comparison of reaction orders, activation energy, pre-exponential factors, and adsorption kinetic parameters due to electrochemical reactions in DRM/SRM-SOFC systems. The literature mentioned above demonstrates that kinetic studies and modeling electrocatalysis effectively predict adsorption parameters, guide experiments, and enhance anode materials for SOFCs, including designing novel electrocatalytic materials for improved performance.

Most studies on adsorption kinetic on SOFC anodes have focused on Langmuir kinetic models, along with specifically defined formulas, which have been employed to describe adsorption behavior at equilibrium. In contrast, there has been no discussion on how current density and temperature influence adsorption thermodynamic properties, including the Gibbs free adsorption energy. Calculating the standard Gibbs free energy change for adsorption (ΔG^0_{ad}) values as a function of operation condition of SOFC helps determine the relative ease or difficulty with which reactants adsorb onto the catalyst's surface under given conditions. While the standard Gibbs free energy (ΔG°) is an intrinsic material property [22,23], the apparent adsorption free energy or Gibbs free energy change for adsorption (ΔG^0_{ad}) reported here reflects the operating conditions under electrochemical load [24]. Variations in current density influence surface potential [25]and local reaction environments, which in turn affect the fitted adsorption equilibrium constants [7,13]. This results in a shift in ΔG^0_{ad}, consistent with literature on potential-dependent adsorption in electrochemical systems [26–28]. If oxidant molecules (CO_2 or H_2O) have a lower ΔG^0_{ad}, they will preferentially adsorb onto the catalyst, potentially leading to higher reaction rates. This is because of the ΔG^0_{ad} can be assessed using a dimensionless thermodynamic equilibrium constant, which measures the spontaneity of an adsorption process, with more negative values indicating greater energetic favourability. For instance, at a specific reaction temperature,

the adsorption process can be spontaneous ($\Delta G^0_{ad} < 0$) or non-spontaneous ($\Delta G^0_{ad} > 0$). Applying the first and second laws of thermodynamics, coupled with adsorption isotherms models, provides a straightforward description of electrocatalysis and adsorption behavior inside SOFCs. This area still lacks sufficient research. No available study elucidates the Gibbs free energy changes of adsorption associated with CO_2 and H_2O species over SOFCs. This gap exists due to the complexity of SRM and DRM, which involve numerous side reactions, such as the reverse water gas shift reaction (RWGS), methane cracking, and the Boudouard reaction [5]. Both processes inevitably cause carbon deposits beside associated electrochemical reactions, significantly affecting these side reactions during methane reforming [29]. Furthermore, the multitude of elementary reactions involved, which leads to a complex reaction network, makes it challenging to accurately determine the adsorption energies and other kinetic parameters of all possible reaction intermediates using the Density Functional Theory (DFT) method. Considering the explanations above, we hypothesize that thermodynamic adsorption properties can provide valuable insights into the mechanism of spontaneous or non-spontaneous adsorption processes in DRM/SRM-SOFC systems.

In studies of physisorption (physical adsorption) and chemisorption (chemical adsorption) thermodynamics, the equilibrium constants derived from adsorption isotherm models are frequently utilized to determine ΔG^0_{ad}, enthalpy (ΔH^0_{ad}), and entropy (ΔS^0_{ad}) of adsorption [30]. The standard Gibbs free energy change for adsorption ΔG^0_{ad} is critical in understanding their behavior and competition with CH_4 in electrocatalytic reactions during the steps of oxidant molecules adsorption [23]. ΔG^0_{ad} is determined using the following equation:

$$\Delta G^0_{ad} = -RT \ln K_{ads} \tag{1}$$

In this formula, K_{ads} represents the unitless thermodynamic equilibrium constant, T is the absolute temperature in kelvins, and R is the gas constant, valued at 8.314 J mol^{-1} K^{-1}. The connection between ΔG^0_{ad}, ΔH^0_{ad}, and ΔS^0_{ad} of adsorption is given by Ref. [31]:

$$\Delta G^0_{ad} = \Delta H^0_{ad} - T\Delta S^0_{ad} \tag{2}$$

By combining these equations, the relationship becomes:

$$\ln K_{ads} = -\left(\frac{1}{T}\right)\frac{\Delta H^0_{ad}}{R} + \frac{\Delta S^0_{ad}}{R} \tag{3}$$

A plot of ln K_{ads} versus 1/T yields a straight line, from which ΔH^0_{ad} and ΔS^0_{ad} can be determined based on the slope and intercept of the van't Hoff equation, based on the first and second laws of thermodynamics [32]. An endothermic process is indicated by a positive ΔH^0_{ad}, while a negative ΔH^0_{ad} indicates an exothermic process. Additionally, the magnitude of ΔH^0_{ad} provides information on the type of adsorption which $\Delta H^0_{ad} \leq 60$ kJ/mol suggest physisorption, while $\Delta H^0_{ad} \geq 200$ kJ/mol indicate chemisorption [33]. A low ΔS^0_{ad} value generally signifies minimal entropy change during adsorption, whereas a positive ΔS^0_{ad} suggests increased randomness at the catalyst interface. Researchers have found that an efficient adsorption of species over an electrocatalyst should have a ΔG^0_{ad} value close to zero [34]. When ΔG^0_{ad} equals zero, maximum adsorption activity can be achieved. A more negative ΔG^0_{ad} value indicates stronger binding between reactants and the catalyst surface, hindering product desorption. Conversely, a more positive ΔG^0_{ad} value results in weaker binding, impeding the proton/electron-transfer step. ΔG^0_{ad} also indicate the minimum necessary work to load the adsorbents to a certain level in an isothermal path [35]. Since the adsorption of reactants involved in DRM and SRM is considered to be physisorption [29], and this describes the activity of oxidant species and their competition with methane molecules for occupying active sites in electrocatalytic reactions, the Gibbs free energy changes of oxidants is a valuable factor in the initial stages of anode development.

Thermodynamic functions, such as Gibbs free energy, provide a complete system description. However, the presence of an electrical field is consistent with changes in free energy, which include both energetic and entropic contributions [36]. Within the academic community, perceptions regarding the outcomes of the DFT method do not always accurately reflect its true capabilities and limitations [37]. Currently, no experimental method can measure the total amount of gas adsorbed in the anode surface pores during high-temperature electrochemical reactions over SOFCs. The volumetric technique cannot differentiate between gas in the anode pores and the gas phase, while the gravimetric method requires a buoyancy correction that prevents accurate measurement [36]. Furthermore, thermodynamic simulation tools can determine the overall Gibbs free energy of reactions as a function of temperature and pressure, utilizing data from experimental studies [38]. However, these methods fail to explain the phenomena occurring inside electrochemical devices like SOFCs when electrochemistry and associated current density are involved in reaction kinetics. Simultaneously, theoretical research on the dissociation reactions of reactants related to DRM and SRM on anode surfaces in SOFCs is becoming increasingly precise. Nonetheless, the study of the Gibbs free energy of oxidants in SOFCs remains in its early stages, and several critical questions still need to be addressed, including the effects of current density on the Gibbs free energy of adsorption of oxidants' species. This study addresses the above questions using available methods and data in the literature and fitting the data based on the Arrhenius Equation.

2. Methodology

This study employs the Langmuir adsorption model to evaluate the equilibrium characteristics of CH_4, CO_2, and H_2O adsorption under varying temperature and current density conditions. To validate the thermodynamic predictions, a combination of density functional theory (DFT) simulations and experimental adsorption measurements using temperature-programmed desorption (TPD) techniques were incorporated. These methods provide insights into the energy barriers associated with surface reactions and confirm theoretical findings with empirical data [40].

The experimental data in this study were obtained from a commercial type of button fuel cell with an electrolyte-supported design featuring Hionic™ electrolyte that serves as both structural support and a sealing surface. The cathode comprises a multi-layered LSM-GDC/LSM structure, while the anode consists of a multi-layered NiO-GDC/NiO-YSZ structure, as described in our previous research [9]. The structure of the SOFC button cell [39] is illustrated in Fig. 1.

In the SOFCs, the Triple Phase Boundary (TPB) in the anode is a critical region where the electrolyte, the anode material, and the fuel gas come into contact. The electrolyte, typically a ceramic material like yttria-stabilized zirconia (YSZ), conducts oxygen ions [41]. The fuel gas reacts on the anode material, such as a composite of nickel (Ni) and YSZ [8]. The TPB is essential for the electrochemical reactions that generate electricity in an SOFC [13]. At the TPB, oxygen ions from the electrolyte diffuse to the boundary, fuel molecules from the gas phase are adsorbed onto the anode surface, and electrons released from the oxidation of the fuel at the anode flow through the external circuit to the cathode [7]. This highlights the necessity of all three phases being in contact. The efficiency and performance of the anode are significantly influenced by the density and length of these TPBs, as they provide active sites for the electrochemical reactions [21]. Consequently, the design and material choice for the anode are crucial to maximize TPB length and ensure efficient fuel oxidation and ion conduction [41]. This is because a high specific surface area, pore volume, and porosity of the support facilitate the dispersion of a large amount of highly reducible NiO and ensure reasonable anode basicity. These factors ultimately lower the activation energy, enhance the catalyst activity, reduce the coke deposition, and

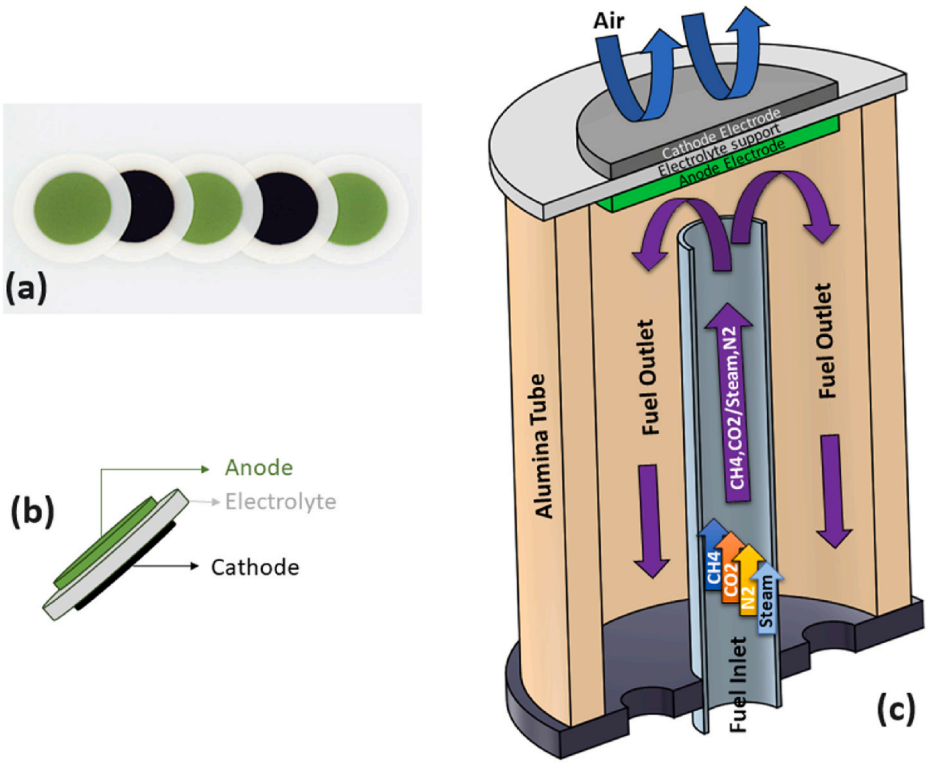

Fig. 1. (a) NextCell™ electrolyte-supported button cell [39], (b) button cell structure and (c) experimental set up consist of alumina tube attached to button cell, fuel inlet and outlet configuration.

increase the catalyst stability.

In theoretical adsorption systems involving porous materials, the system is typically depicted as comprising two main macroscopic phases: a gas phase and a solid phase. This solid phase can be considered the TPB in SOFC. The electrode's surface, which includes metal catalysts and ceramic support, is designed to be porous, conductive, and catalytically active [8]. To distinguish between reactant molecules in these phases, it is necessary to differentiate between those adsorbed on the surface and those in the gas phase. For instance, a molecule close to the anode surface might still be considered part of the gas phase. Josiah Willard Gibbs addressed this challenge by introducing the concept of the dividing surface in his interface model. The Gibbs model uses the concept of excess quantities, such as energy and entropy, to describe how properties at the interface differ from those in the bulk phases [42,

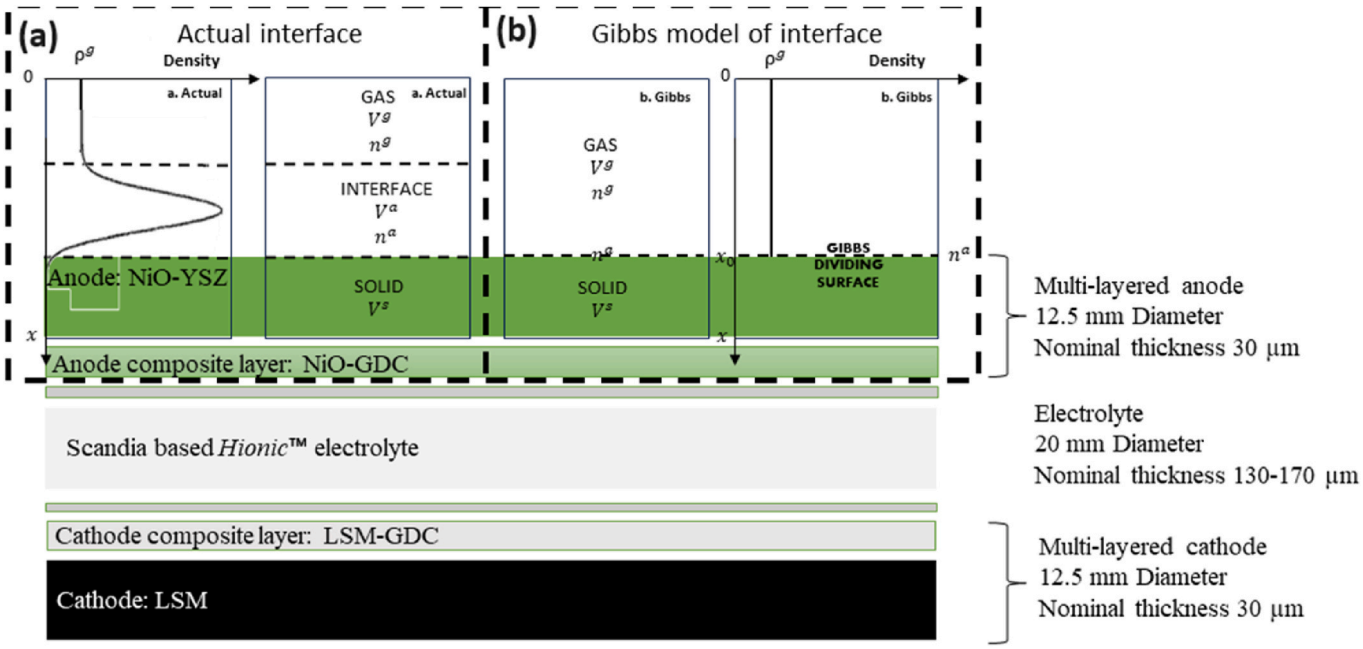

Fig. 2. Detailed electrolyte-supported button cell structure and gas density profile at gas-anode interface. (a) the actual density profile near the surface, and (b) the Gibbs model [36,39].

43]. Gibbs proposed the idea of an imaginary dividing surface to separate the two phases and measure these excess properties, with its position chosen to simplify calculations, such as by setting the excess number of molecules to zero [36,44]. Fig. 2 shows the detailed structure of the electrolyte-supported button cell alongside the previously mentioned gas density profile at the gas-anode interface, providing a comprehensive view of the cell's architecture and interface behavior [36]. Section (a) in Fig. 2 shows the density profile in a single-component adsorption system, where adsorbate density is constant in the gas phase and zero in the solid phase. The dividing surface's location affects the amount of adsorbate at the interface. Section (b) in Fig. 2 illustrates the Gibbs model, which represents the interface with a single idealized dividing surface and a uniform gas phase density up to this surface.

The cell had a geometric area of 0.95 cm^2 and a thickness of 30 μm. Electrical contacts were made using silver wires bonded with silver SOFC ink. The button cell was attached to an alumina tube using high-temperature ceramic adhesives, with fuel gas delivered through a smaller alumina tube directly to the anode. The anode was initially heated to 1073 K in a nitrogen atmosphere at a rate of 2 K/min. The flow rates were controlled using mass flow controllers, maintaining a total flow rate of 8 nml/min at P = 1 bar. After a 4-h reduction in pure H_2, the hydrogen was substituted with various biogas compositions detailed in supplementary material. Experiments were conducted at 973 K, 1023 K, and 1073 K, with current densities set at 0, 500, and 1000 A/m^2 using an electrochemical impedance analyzer (EIS) under galvanostatic conditions. Moisture from the anode off-gas was removed via a condenser and silica gel desiccant bed. The dehydrated syngas were analyzed using a gas chromatograph with a thermal conductivity detector calibrated with known gas compositions. Gas measurements were taken once the cell temperature and voltage stabilized, typically after 18 h of continuous operation, ensuring consistent gas composition, current density, and temperature. For further details on the cell design and experimental methodology, please refer to our previous studies [4,9]. The overall methane conversion (x_{CH_4}) at the anode off-gas outlet is determined by Equation (1):

$$x_{CH_4} = \frac{F_{CH_4}^{inlet} - F_{CH_4}^{outlet}}{F_{CH_4}^{inlet}} \quad (1)$$

where $F_{CH_4}^{inlet}$ and $F_{CH_4}^{outlet}$ are the CH_4 flow rates at the inlet and outlet, respectively. The methane conversions collected at various temperatures, current densities, and gas compositions will be used to fit in the Langmuir kinetics model. In this continuously flowing SOFC system, equilibrium properties were not directly measured but inferred under steady-state conditions using outlet gas compositions and fitted kinetic models, assuming local equilibrium for reversible steps [45,46]. For a comprehensive understanding of the governing equations and the methodology for mathematical modeling, readers are encouraged to refer to our previous studies [4,9,13]. The Langmuir adsorption isotherm model was utilized to estimate the adsorption energy of the primary species involved in the DRM and SRM processes, alongside other parameters including K_{ads}, ΔH_{ad}^0, and ΔS_{ad}^0. Finally, ΔG_{ad}^0 was calculated iteratively in MATLAB, as detailed in the Supplementary Material.

3. Results and discussion

The Gibbs free energy of oxidant adsorption is considered the key factor in determining the reforming reaction activity of an electrocatalyst [34]. The developed thermodynamic method for internal reforming inside SOFCs needs to be tested using Gibbs free energy of adsorption parameters to ensure its applicability in anode development stages. The objectives of the present study are as follows:

1. Implement the Langmuir kinetic model for internal DRM and SRM within SOFCs to calculate the thermodynamic properties of adsorption.
2. Compare the competition between oxidant species and methane to occupy active sites on the anode surface under varying process conditions (i.e., temperature and current density).
3. Characterize the thermodynamic behavior of adsorbate components on the anode and validate its application in the anode development stage for SOFC applications.

The initial section of this research examines the influence of operational parameters on the Gibbs free energy change of adsorption of oxidant species. The subsequent section explores how operation variables affect the adsorption constant ratio of methane to oxidants. Table 1 shows the derived kinetic parameters for the Langmuir adsorption isotherm model under different temperature and current density conditions. The data were adapted from S. Moarrefi et al. [9], which investigated internal dry reforming and steam reforming within a SOFC using a NiO-GDC-YSZ anode, LSM/LSM-GDC cathode, and a Hionic™ scandium-stabilized zirconia electrolyte. These values were used to support model calculations and enable performance comparisons in the present study.

3.1. Influence of operation conditions on Gibbs free energy ΔG° of adsorption

As mentioned in previous sections, understanding the simultaneous effects of temperature, current density, and ΔG_{ad}^0 of CO_2 and H_2O species is crucial for optimizing the anode. A detailed analysis of these interactions provides insight into the electrocatalytic behavior of SOFCs under different operating conditions [47]. The 3D plot depicted in Fig. 3 (e)–(f) provides a comprehensive view of these interactions, allowing for better comparison and analysis (see Fig. 4).

Comparing the ΔG_{ad}^0 magnitude of CO_2 and H_2O adsorption in Fig. 3 (a) and (b) reveals that H_2O molecules exhibit lower ΔG° values than CO_2 under identical process conditions, approaching nearly zero. This indicated higher adsorption activity for H_2O and more favorable adsorption than CO_2. Nevertheless, in the anode development stage, analyzing ΔG° magnitude of oxidant species over different anode designs provide an accurate measurement to verify anode performance. From Fig. 3(a) and (b), it is evident that as temperature rises, the ΔG° increases for both oxidants, indicating a reduction in adsorption spontaneity. This observation suggests that higher temperatures lead to a more positive ΔG° value for both oxidants, weakening their binding to the surface and increasing their desorption frequency. This phenomenon promotes the formation of syngas products. This weaker binding can also delay the proton/electron-transfer step and reduce the efficiency of species adsorption over the electrocatalyst, particularly when the ΔG° value deviates further from zero. The differences in ΔG° from 973K to 1073K, as shown in Fig. 3(c) and (d), indicate that the temperature induces changes of a similar magnitude in ΔG° for both species. This observation aligns with previous studies on thermodynamic equilibrium in high-temperature fuel cells, where increased temperature enhances the desorption frequency of oxidants and promotes syngas formation. However, a notable implication is the potential increase in carbon deposition, particularly in DRM, where CO_2 adsorption is relatively weaker. Studies indicate that excessive CO_2 desorption can lead to carbon formation via the Boudouard reaction, emphasizing the need for a balanced oxidation mechanism in the anode [1,2,38,48].

Increased electrical load affects the adsorption process differently for steam and carbon dioxide species, as shown in Fig. 3(a) and (b). For the CO_2 component, the ΔG° adsorption reaches its maximum value around a current density of 600 A/m^2 and decreases as more current is drawn from the cell. This phenomenon indicates that higher current density weakens binding to the surface and impedes the proton/electron-

Table 1
Derived kinetic parameters for Langmuir adsorption isotherm model at different temperatures and current densities [9].

Kinetic Parameters	Temperature (K)	973	1023	1073	973	1023	1073	973	1023	1073
	Current Density [A/m^2]	CH_4			H_2O (SRM)			CO_2 (DRM)		
K_j	**Open-Circuit**	0.075	0.060	0.049	0.97	0.76	0.61	8.7E-08	8.4E-08	8.0E-08
	500	0.075	0.060	0.049	0.60	0.48	0.39	5.2E-09	5.0E-09	4.8E-09
	1000	0.075	0.060	0.049	0.54	0.43	0.36	1.5E-08	1.4E-08	1.4E-08
ΔG_j^0 (kJ/mol. K)	**Open-Circuit**	–	–	–	0.2	2.3	4.4	131.5	138.6	145.7
	500	–	–		4.1	6.2	8.3	154.3	162.6	170.9
	1000	–	–	–	5.0	7.1	9.2	145.7	153.6	161.4

transfer step up to a specific current density level, after which the adsorption process for CO_2 molecules becomes more spontaneous with further current drawn from the cell. This suggests that electrochemical polarization effects alter CO_2 adsorption kinetics, potentially modifying surface reaction pathways. In contrast, for H_2O species, the adsorption ΔG° increases with current density but reaches a maximum and plateaus at higher current densities. This plateau, observed within the current density range investigated in this study, suggests that further increasing the current density does not significantly alter the ΔG° value for water molecules in the SRM process under comparable operating conditions to those in DRM. This behavior is linked to electrochemical interactions at the anode surface. Studies suggest that an external electric field influences the adsorption enthalpy (ΔH) of surface species, leading to a shift in equilibrium constants favoring H_2O over CO_2. This aligns with the experimental observation that SOFCs operating at higher current densities promote steam adsorption, further reinforcing SRM's superior performance in preventing carbon deposition [3,4,49].

In our study, the 3D plots in Fig. 3(e) and (f) reveal distinct regions where CO_2 and H_2O species exhibit varying adsorption spontaneity. Specifically, H_2O species demonstrate less energetically favorable adsorption at higher temperatures and current densities. In contrast, CO_2 exhibits lower spontaneity of adsorption at moderate current densities and elevated temperatures. Additionally, as temperature rises, the absolute values of ΔG° for H_2O and CO_2 increase, indicating that higher temperatures benefit the adsorption process. These findings provide valuable insights into the behavior of adsorbed species in the context of our research.

3.2. Influence of operation conditions on adsorption equilibrium constant

The adsorption equilibrium constant (K_{ads}) quantifies the interaction strength between an adsorbate and the anode surface therefore plays a crucial role in determining the relative affinity of oxidants and fuel molecules for active sites on the anode surface. This constant is influenced by several operational parameters, including temperature, current density, and fuel composition. Understanding these influences can aid in optimizing SOFC performance and minimizing degradation mechanisms. In this study, adsorption equilibrium constants were evaluated at different current densities (0, 500, and 1000 A/m^2) and temperatures (973, 1023, and 1073 K) to analyze how operational factors influence reforming efficiency.

The adsorption equilibrium constant for CH_4 remains relatively constant across different current densities at each temperature. At 973 K, 1023 K, and 1073 K, CH_4 adsorption equilibrium values are approximately 0.075, 0.060, and 0.049, respectively. This suggests that CH_4 adsorption is more sensitive to temperature than to current density, indicating that thermal effects dominate over electrochemical influence in methane reforming. Unlike CH_4, CO_2 adsorption equilibrium constants decrease significantly with increasing current density, suggesting a strong influence of electrochemical potential on CO_2 affinity. At 1073 K, the equilibrium constant drops from 8.034E-08 (open circuit) to 1.385E-08 at 1000 A/m^2, showing that higher electrical loads weaken CO_2 adsorption. This behavior aligns with prior studies, which suggest that electrochemical polarization reduces CO_2 adsorption strength due to competitive surface interactions [48,50]. A similar trend is observed for H_2O adsorption, where the equilibrium constant decreases with increasing temperature and current density. At 973 K, the constant declines from 0.973 (open circuit) to 0.539 at 1000 A/m^2. Similarly, at 1073 K, it drops from 0.609 to 0.357, indicating reduced H_2O adsorption under higher thermal and electrical loads [7,51].

The findings suggest that temperature plays a dominant role in CH_4 adsorption, while current density has a stronger effect on CO_2 and H_2O adsorption behaviors. The reduced CO_2 and H_2O adsorption at high current densities can be attributed to electrochemical polarization effects, which alter the surface charge distribution and modify adsorption affinity. Moreover, the declining adsorption equilibrium constants for all species at higher temperatures highlight the importance of optimizing operating conditions to prevent excessive desorption and ensure efficient fuel conversion. Future studies should explore how modifying anode surface properties—such as nanostructured catalysts or doped perovskites—can stabilize adsorption equilibrium under high-temperature and high-current-density conditions [47,52].

Moreover, numerous studies [4,7,8,21] prove that K_{ads} of CH_4, CO_2, and H_2O on the anode vary depending on the support structure. Mathematically, adsorption constant ratio is defined as the ratio of the forward rate constant for adsorption to the reverse rate constant for desorption. A high K_{ads} value indicates strong adsorption, suggesting that reactants are more likely to remain on the surface of the anode, facilitating surface reactions [4]. Conversely, a low K_{ads} value indicates weak adsorption, with reactants more likely to desorb quickly without reacting. Understanding this ratiois crucial for predicting reaction kinetics on anode surfaces, controlling reaction rates, and predicting reaction pathways, highlighting the close relationship between the adsorption affinity of reactants and anode properties influenced by the support type [13]. However, the ratio of adsorption equilibrium constants for CH_4 and oxidant molecules is a useful measurement parameter that has not yet been investigated in anode research area. The adsorption equilibrium constants for the DRM and SRM processes are defined by the following equations respectively:

$$K_{ad-DRM} = \frac{K_{CH_4}}{K_{CO_2}} \tag{4}$$

$$K_{ad-SRM} = \frac{K_{CH_4}}{K_{H_2O}} \tag{5}$$

This ratio reflects anode reducibility and basicity, which correlate with the activity order in anode development studies. Furthermore, multiple studies reveal that thermodynamic equilibrium can indicate the side-promoting coke formation and can also be used to develop strategies to minimise coke formation [36]. Nevertheless, an anode with low optimal Ni content and excessive basicity may lead to CO_2 and H_2O adsorption compared to CH_4, resulting in coking and reduced catalyst activity. This issue can be investigated parametrically using the adsorption mentioned above constant ratios.

Studies have shown that increasing temperature leads to a shift in the adsorption equilibrium, favoring methane decomposition over oxidant

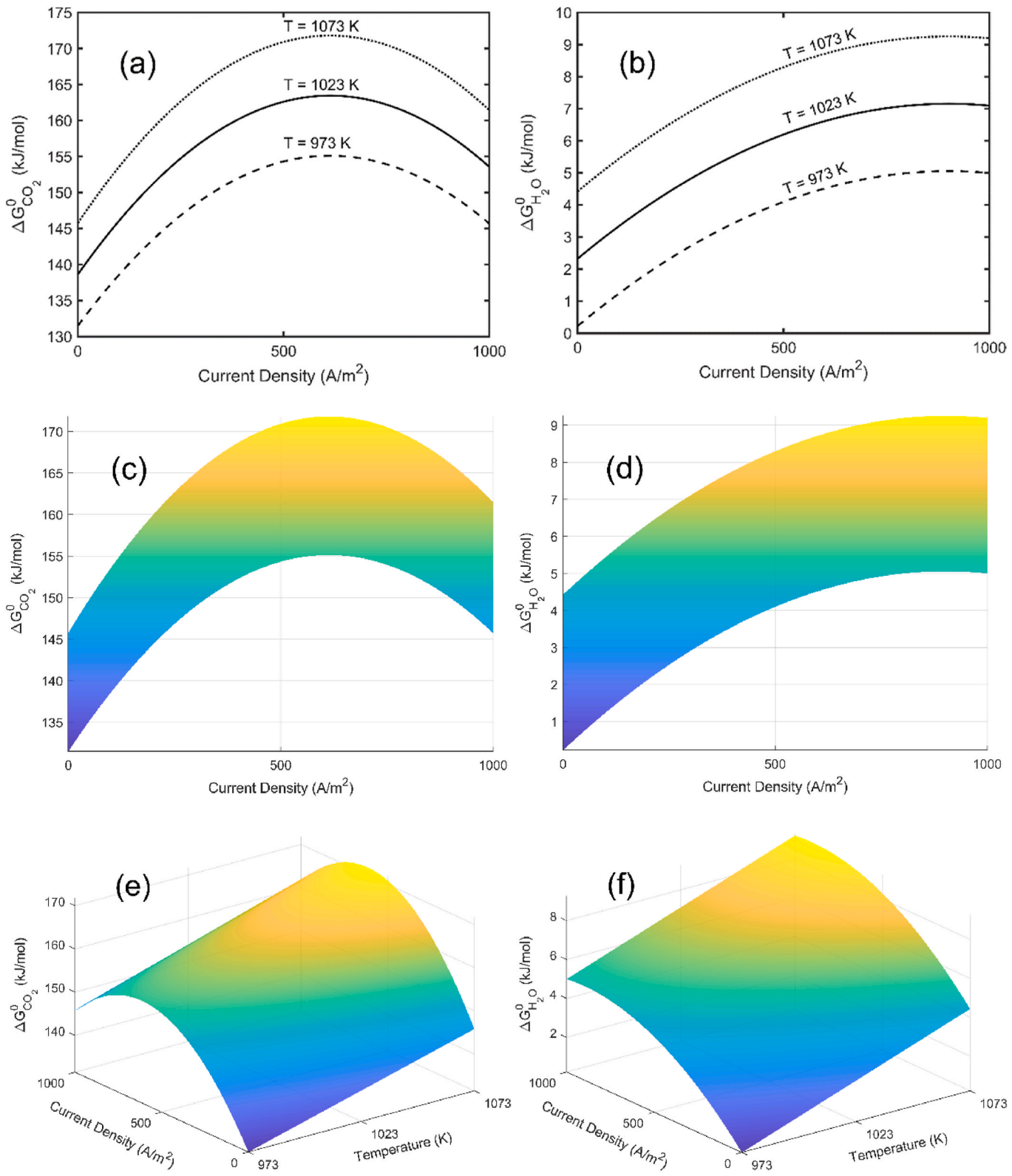

Fig. 3. The impact of current density and temperature on Gibbs free energy of adsorption (ΔG^0_{ad}) of oxidants in each process. (a) ΔG^0_{ad} for CO_2 adsorption; (b) ΔG^0_{ad} for H_2O adsorption; (c) Changes of ΔG^0_{ad} for CO_2 from 973K to 1073K and current density from OCV to 1000 A/m^2; (d) Changes of ΔG^0_{ad} for H_2O from 973K to 1073K and current density from OCV to 1000 A/m^2; (e) 3D plot showing temperature and current density effects on CO_2 adsorption; (f) 3D plot showing temperature and current density effects on H_2O adsorption.

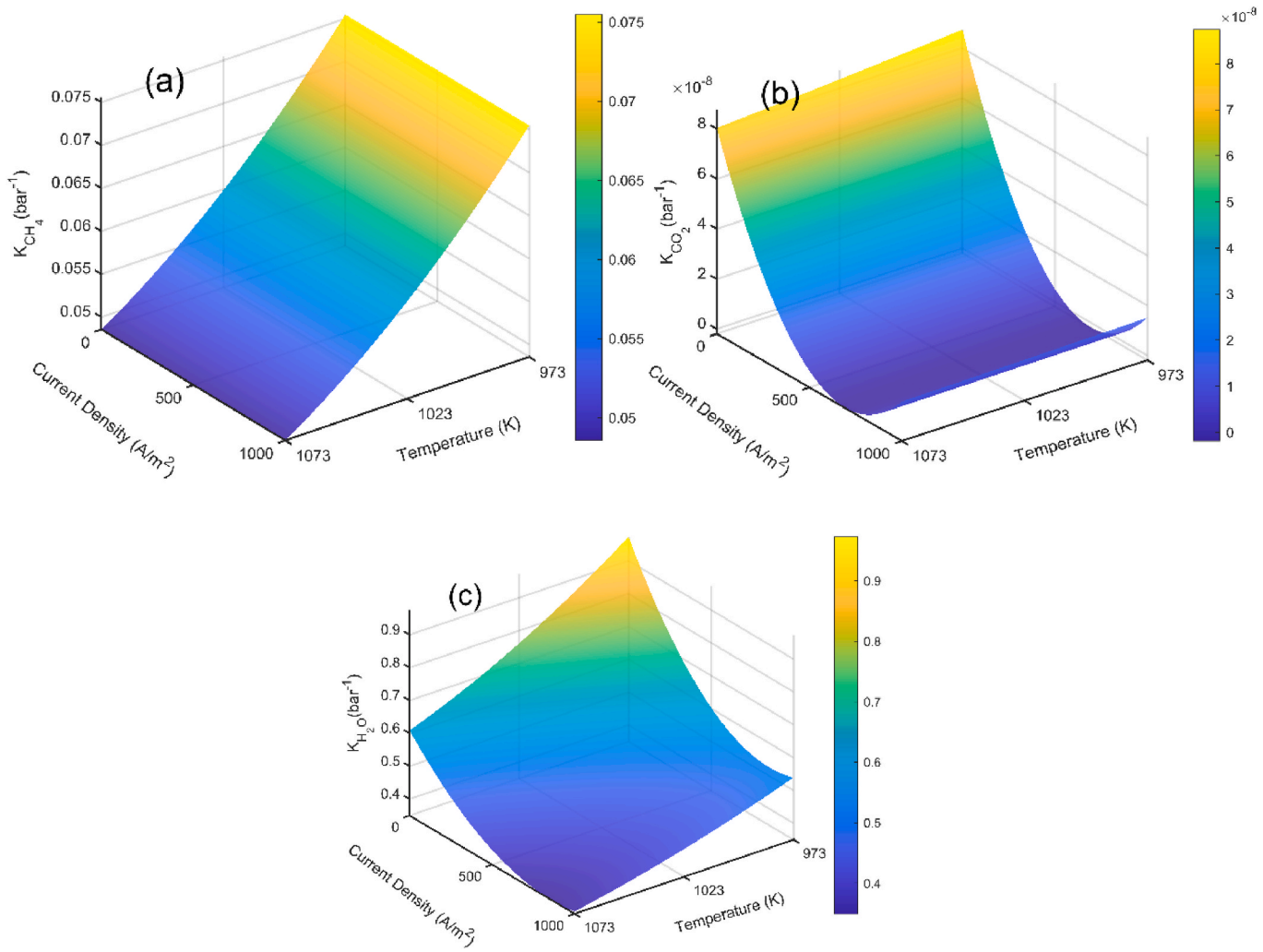

Fig. 4. 3D Surface Plot of Adsorption Equilibrium Constant CH4, CO2 and H2O. This 3D surface plot illustrates the relationship between current density, temperature, and the adsorption equilibrium constant each component. The x-axis represents the current density (in A/m^2), ranging from 0 to 1000 A/m^2. The y-axis denotes the temperature (in K), spanning from 973 K to 1073 K. The z-axis shows the adsorption equilibrium constant values for CH4, CO2 and H2O.

adsorption. This trend is particularly significant in dry reforming conditions, where CO_2 adsorption weakens at high temperatures, potentially increasing carbon deposition risks. Additionally, variations in current density impact the electrochemical potential at the anode-electrolyte interface, altering adsorption behaviors. Higher current densities promote stronger H_2O adsorption, which enhances steam reforming reactions and improves carbon mitigation strategies [53,54]. Fig. 5(a) to 5(f) shows the ratio between the adsorption constants at various current densities and temperatures. In the Langmuir model used in this study, K_{CH4} was assumed to depend only on temperature, a common assumption in similar studies [4,7,13]. This is because methane reforming occurs on or near the anode's outer surface, with CH_4 diffusing from the bulk flow into the anode. [13]. This assumption implies that CH_4 adsorption parameters are independent of current density, while other species in this study are both temperature and current-density dependent. Therefore, as operating conditions change, the adsorption constant ratios vary based on the oxidants' adsorption parameters. As mentioned earlier, as the current density and temperature increase, the adsorption amounts of CO_2 and H_2O on the anode decrease. This phenomenon is due to the exothermic nature of the adsorption process and also the current density effects on temperature gradient over the anode surface [4]. Higher temperatures increase the surface adsorption energy and the molecular diffusion rate, leading to instability in the adsorbed oxidant and CH_4 molecules [31]. Specifically, as current density increases, K_{CO2} and K_{H2O} decrease, increasing the adsorption constant ratio due to lower CO_2 and H_2O adsorption than CH_4, resulting in a higher possibility of carbon formation and lower catalyst activity [17]. The increase in this ratio for both processes is not straightforward, as indicated in Fig. 5(a). The highest ratio for DRM occurs at 500 A/m^2. It decreases with a current density, suggesting that the apparent reaction rate is optimized while coke production is minimized at specific current density levels. This behavior differs in SRM, as illustrated in Fig. 5(b), where the adsorption ratio increases with increasing current density, reaching its maximum and flattening near 1000 A/m^2. This behavior reinforces the superior coking resistance of SRM due to the stronger interaction of H_2O with active sites on the anode [30,49].

These findings highlight the importance of balancing CH_4 and oxidant adsorption for optimal SOFC performance. Anodes with excessive basicity favor oxidant adsorption but may also increase coking risks by inhibiting methane activation. Therefore, achieving an optimal adsorption equilibrium is crucial for ensuring catalyst longevity and efficiency. Most studies concluded that increasing temperature could reduce coke formation according to thermodynamic calculations, as shown in this figure, where an increase in temperature decreases the ratio of adsorption equilibrium. According to Fig. 5(c) and (d), CO_2 adsorption is more temperature dependent than H_2O in the temperature range investigated in this study. However, the small difference between

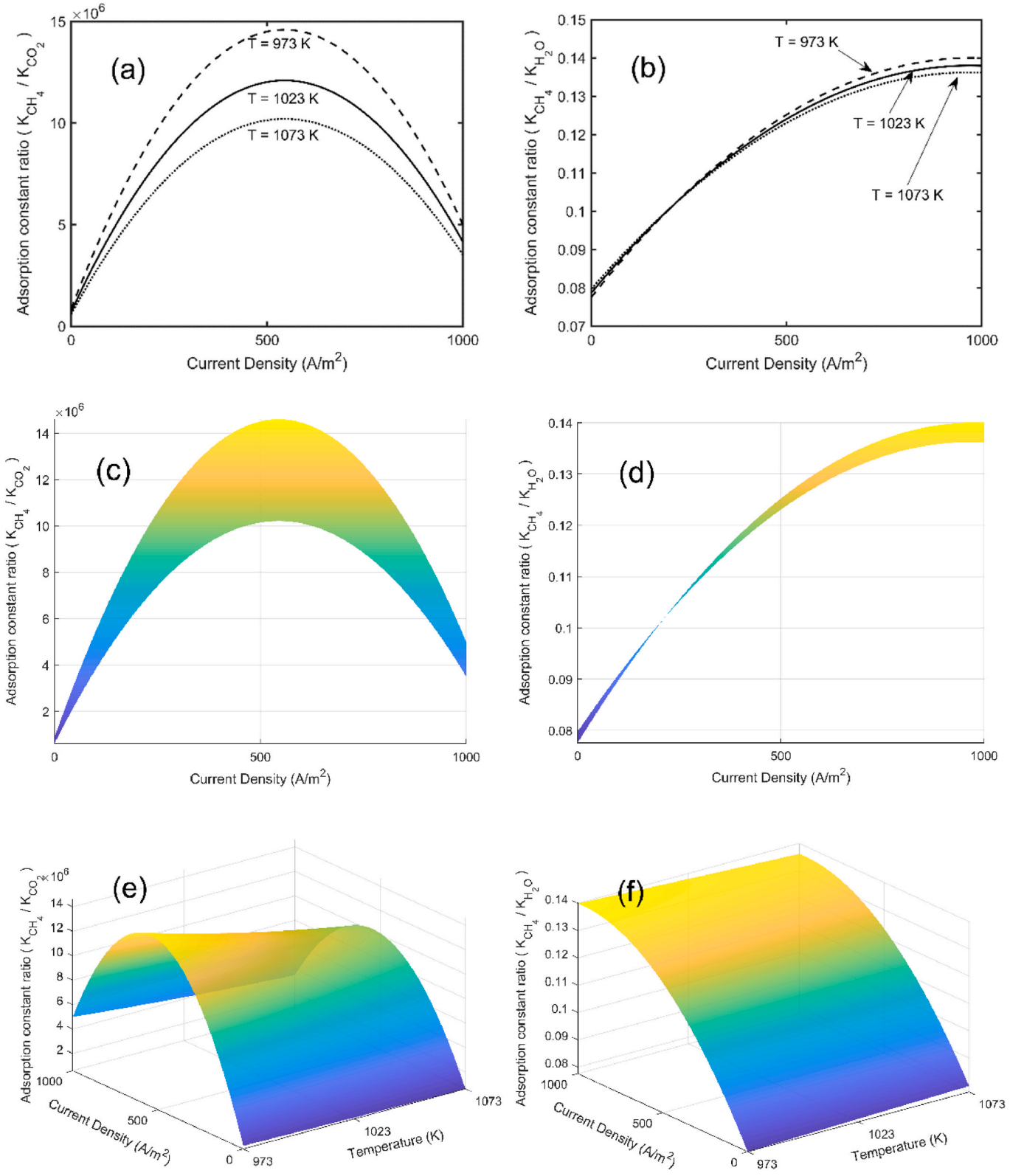

Fig. 5. The impact of current density and temperature on adsorption constant ratio of oxidants in each process. (a) $\frac{K_{CH_4}}{K_{CO_2}}$ for in DRM; (b) $\frac{K_{CH_4}}{K_{H_2O}}$ for SRM; (c) Changes of $\frac{K_{CH_4}}{K_{CO_2}}$ for DRM from 973K to 1073K and current density from OCV to 1000 A/m^2; (d) Changes of $\frac{K_{CH_4}}{K_{H_2O}}$ for SRM from 973K to 1073K and current density from OCV to 1000 A/m^2; (e) 3D plot showing temperature and current density effects on adsorption constant ratio in DRM; (f) 3D plot showing temperature and current density effects on adsorption constant ratio in SRM.

K_{CH4} and K_{H2O} results in lower adsorption constant ratios, lower carbon deposition, and higher catalyst activity for SRM. Therefore, our results confirm that SRM remains a more effective reforming process than DRM in mitigating carbon deposition. This conclusion is supported by previous research demonstrating that SRM-based SOFCs exhibit greater long-term stability than DRM-based counterparts due to the stronger retention of H_2O on the catalyst surface [8]. Based on Fig. 5(e) and (f), we concluded that since two different parameters significantly influence adsorption kinetics, the adsorption constant ratio could be used to investigate catalyst activity and coke formation on the anode for SOFC applications with this method and refining anode design strategies.

Furthermore, the interaction between operating pressure and adsorption kinetics has been explored in recent experimental studies. It has been observed that increasing system pressure improves CH_4 adsorption by enhancing reactant surface coverage. However, excessive pressure can suppress CO_2 adsorption, leading to imbalanced reforming reactions and a higher likelihood of coking [55]. Optimizing operating conditions by balancing temperature, pressure, and fuel composition is therefore critical for ensuring stable long-term SOFC performance.

4. Conclusions

NiO–GDC–YSZ anode materials are a highly significant class of materials, drawing considerable interest from researchers due to their potential in energy conversion for SOFC technologies. Despite their critical role in anode structure for fuel cells, a literature review reveals that these materials' adsorption kinetics and thermodynamics have been insufficiently studied. In this study, we investigated the role of the Gibbs free energy of oxidant adsorption in determining the electrocatalyst activity for SOFCs. Specifically, we explored how these operational parameters affect the Gibbs free energy change of oxidant adsorption and examined the influence of these variables on the adsorption constant ratio of methane to oxidants. This anode consists of both metallic (Ni) and ceramic (YSZ and GDC) phases, each playing a different role in the adsorption and electrochemical processes. Ni acts as the main catalytic site, where CH_4 and H_2 are adsorbed and oxidized, mainly at the triple-phase boundary, where it contacts the electrolyte. YSZ conducts oxygen ions (O^{2-}) but has minimal direct interaction with fuel molecules. GDC, as a mixed ionic–electronic conductor, allows additional surface reactions beyond the TPB, especially under higher current densities where oxygen ion transport is more active. As a result, Ni supports fast catalytic adsorption, while GDC and YSZ contribute indirectly by enabling ion transport and redox reactions. These differences lead to distinct adsorption behaviors across the anode surface. Further studies are needed to fully interpret these effects, but they justify treating CO_2 and H_2O adsorption separately in the kinetic model.

By applying the Langmuir kinetic model, we calculated the thermodynamic properties of adsorption for both internal dry reforming of methane and steam reforming of methane. To optimize the anode, we successfully explored the simultaneous effects of temperature, current density, and the standard Gibbs free energy change (ΔG°) of CO_2 and H_2O species. Our analysis revealed that H_2O exhibits lower ΔG° values than CO_2 under identical process conditions, indicating more favorable adsorption and higher adsorption activity for H_2O. As temperature increases, ΔG° for both CO_2 and H_2O becomes more positive, weakening their surface binding and increasing desorption frequency, promoting syngas product formation. Additionally, we observed that higher temperatures and current densities affect the adsorption process differently for CO_2 and H_2O, with CO_2 showing reduced adsorption at high current densities, while H_2O adsorption increases and reaches a plateau at higher current densities. Our 3D plots provided insights into how temperature and current density influence the adsorption behavior of CO_2 and H_2O, revealing that higher temperatures favor the adsorption process, though they also increase the ΔG° values for both species. Furthermore, we introduced a novel approach to comparing carbon deposition probabilities by analyzing the adsorption equilibrium constant ratios for CO_2 and H_2O with CH_4 during DRM and SRM processes. Our results also confirmed that SRM is more effective than DRM at mitigating coke formation under the same conditions. We found that the adsorption equilibrium constant ratio, which reflects the anode's reducibility and basicity, provides a valuable metric for optimizing anode design and minimizing coke formation. Additionally, we identified that CO_2 adsorption is more temperature-dependent than H_2O, which influences the overall adsorption constant ratios and catalyst performance. Our analysis confirmed that understanding the competition between oxidant species and methane for active sites on the anode surface can be a crucial parameter for optimizing SOFC performance across various operational conditions, including temperature and current density.

Overall, this study provides a straightforward and effective method for evaluating the adsorption behavior of CO_2 and H_2O species and comparing their roles in the DRM and SRM processes. Our findings offer a foundation for future research to improve anode performance in SOFC applications through optimized reaction conditions and a better understanding of adsorption dynamics.

CRediT authorship contribution statement

Saeed Moarrefi: Writing – original draft, Visualization, Validation, Software, Methodology, Investigation, Formal analysis, Data curation. **Mohammad Rajabi Naraki:** Software, Methodology, Investigation. **Mohan Jacob:** Supervision. **Nilay Shah:** Supervision. **Stephen Skinner:** Supervision. **Lichao Jia:** Writing – review & editing. **Shou-Han Zhou:** Writing – review & editing, Software, Investigation. **Weiwei Cai:** Writing – review & editing, Supervision. **Liyuan Fan:** Writing – review & editing, Supervision, Resources, Project administration, Investigation, Funding acquisition, Conceptualization.

Declaration of competing interest

The authors declare that they have no known competing financial interests or personal relationships that could have appeared to influence the work reported in this paper.

Acknowledgement

The authors would like to thank James Cook University, Australia, for providing the education and resources support. This research received no specific grant from funding agencies in the public, commercial, or not-for-profit sectors.

The authors would like to thank The International Collaboration for Hydrogen Research Program, Australia, for supporting the international collaboration.

Nomenclature

Abbreviations	
DRM	Dry Reforming of Methane
SRM	Steam Reforming of Methane
DFT	Density Functional Theory
LH	Langmuir-Hinshelwood
RWGS	Reverse Water Gad Shift
SOFC	Solid Oxide Fuel Cell
NiO-YSZ	Nickel-Yttria-Stabilized-Zirconia
NiO-GDC	Nickel-Gadolinium-Doped-Ceria
PL	Power Law
LSM	lanthanum strontium manganite
TPB	Triple Phase Boundary
Latin symbols	
R	Universal gas constant, 8.314 J/(mol K)
T	Temperature, K
Subscripts	
x_{CH_4}	Overall methane conversion
$F_{CH_4}^{inlet}$	Methane flow rate at the inlet, ml/min
$F_{CH_4}^{outlet}$	Methane flow rate at the outlet, ml/min
K_j	Adsorption equilibrium constant of species j
ΔH_j^0	The change of adsorption enthalpy of species j
ΔS_j^0	The change of entropy of species j
ΔG_j^0	Change of standard Gibbs free energy of adsorption
K_{ads}	Adsorption equilibrium constant

Appendix A. Supplementary data

Supplementary data to this article can be found online at https://doi.org/10.1016/j.jpowsour.2025.237905.

Data availability

Data will be made available on request.

References

[1] Z. Liang, J. Wang, K. Ren, Z. Jiao, M. Ni, L. An, Y. Wang, J. Yang, M. Li, Discovering two general characteristic times of transient responses in solid oxide cells, Nat. Commun. 15 (1) (2024) 4587, https://doi.org/10.1038/s41467-024-48785-1.

[2] A. Ozden, F.P. García de Arquer, J.E. Huang, J. Wicks, J. Sisler, R.K. Miao, C. P. O'Brien, G. Lee, X. Wang, A.H. Ip, E.H. Sargent, D. Sinton, Carbon-efficient carbon dioxide electrolysers, Nat. Sustain. 5 (7) (2022) 563–573, https://doi.org/10.1038/s41893-022-00879-8.

[3] I. Sullivan, A. Goryachev, I.A. Digdaya, X. Li, H.A. Atwater, D.A. Vermaas, C. Xiang, Coupling electrochemical CO2 conversion with CO2 capture, Nat. Catal. 4 (11) (2021) 952–958, https://doi.org/10.1038/s41929-021-00699-7.

[4] S. Moarrefi, M. Jacob, C.e. Li, W. Cai, L. Fan, Internal dry reforming of methane in solid oxide fuel cells, Chem. Eng. J. 489 (2024) 151281, https://doi.org/10.1016/j.cej.2024.151281.

[5] H.H. Faheem, B. Britt, M. Rocha, S.-H. Zhou, C.e. Li, W. Cai, L. Fan, Sensitivity analysis and process optimization for biomass processing in an integrated gasifier-solid oxide fuel cell system, Fuel 356 (2024) 129529, https://doi.org/10.1016/j.fuel.2023.129529.

[6] S. Koohfar, M. Ghasemi, T. Hafen, G. Dimitrakopoulos, D. Kim, J. Pike, S. Elangovan, E.D. Gomez, B. Yildiz, Improvement of oxygen reduction activity and stability on a perovskite oxide surface by electrochemical potential, Nat. Commun. 14 (1) (2023) 7203, https://doi.org/10.1038/s41467-023-42462-5.

[7] L. Fan, A. Mokhov, S.A. Saadabadi, N. Brandon, P.V. Aravind, Methane steam reforming reaction in solid oxide fuel cells: influence of electrochemical reaction and anode thickness, J. Power Sources 507 (2021) 230276, https://doi.org/10.1016/j.jpowsour.2021.230276.

[8] L. Fan, C.e. Li, P.V. Aravind, W. Cai, M. Han, N. Brandon, Methane reforming in solid oxide fuel cells: challenges and strategies, J. Power Sources 538 (2022), https://doi.org/10.1016/j.jpowsour.2022.231573.

[9] S. Moarrefi, M. Jacob, N. Shah, S. Skinner, W. Cai, L. Fan, Comparison of steam and dry reforming adsorption kinetics in solid oxide fuel cells, Fuel 388 (2025) 134413, https://doi.org/10.1016/j.fuel.2025.134413.

[10] H.H. Faheem, S.Z. Abbas, A.N. Tabish, L. Fan, F. Maqbool, A review on mathematical modelling of direct internal Reforming- solid oxide fuel cells, J. Power Sources 520 (2022) 230857, https://doi.org/10.1016/j.jpowsour.2021.230857.

[11] T. Ishihara, Perovskite Oxide for Solid Oxide Fuel Cells 1ed, Springer, New York, 2009, https://doi.org/10.1007/978-0-387-77708-5.

[12] M. Bilal Hanif, M. Motola, S. qayyum, S. Rauf, A. khalid, C.-J. Li, C.-X. Li, Recent advancements, doping strategies and the future perspective of perovskite-based solid oxide fuel cells for energy conversion, Chem. Eng. J. 428 (2022) 132603, https://doi.org/10.1016/j.cej.2021.132603.

[13] S.-H. Zhou, E. Omanga, A.N. Tabish, W. Cai, L. Fan, Effect of electrochemical reaction on steam adsorption during methane reforming on a Ni-GDC anode, Fuel 332 (2023) 125973, https://doi.org/10.1016/j.fuel.2022.125973.

[14] A. Thallam Thattai, L. van Biert, P.V. Aravind, On direct internal methane steam reforming kinetics in operating solid oxide fuel cells with nickel-ceria anodes, J. Power Sources 370 (2017) 71–86, https://doi.org/10.1016/j.jpowsour.2017.09.082.

[15] M. Yusuf, M. Beg, M. Ubaidullah, S.F. Shaikh, L.K. Keong, K. Hellgardt, B. Abdullah, Kinetic studies for DRM over high-performance Ni–W/Al2O3–MgO catalyst, Int. J. Hydrogen Energy 47 (100) (2022) 42150–42159, https://doi.org/10.1016/j.ijhydene.2021.08.021.

[16] Y. Li, Y. Wang, J. Wu, S. Gao, B. Zhu, J. Wang, J. Zhao, L. Wu, L. Zheng, X. Zhang, Catalytic performance of NixCoy catalysts supported on honeycomb-lantern-like CeO2 for dry reforming of methane: synergistic effect and kinetic study, Chem. Eng. Sci. 291 (2024) 119906, https://doi.org/10.1016/j.ces.2024.119906.

[17] T. Nguyen, C.L. Luu, H.P. Phan, P.A. Nguyen, T.T. Van Nguyen, Methane dry reforming over nickel-based catalysts: insight into the support effect and reaction kinetics, React. Kinet. Mech. Catal. 131 (2) (2020) 707–735, https://doi.org/10.1007/s11144-020-01876-8.

[18] L. van Biert, K. Visser, P.V. Aravind, Intrinsic methane steam reforming kinetics on nickel-ceria solid oxide fuel cell anodes, J. Power Sources 443 (2019) 227261, https://doi.org/10.1016/j.jpowsour.2019.227261.

[19] D. Zambrano, J. Soler, J. Herguido, M. Menéndez, Kinetic study of dry reforming of methane over Ni–Ce/Al2O3 catalyst with deactivation, Top. Catal. 62 (5) (2019) 456–466, https://doi.org/10.1007/s11244-019-01157-2.

[20] M.A. Alsaffar, B.V. Ayodele, J.M. Ali, M.A. Abdel Ghany, S.I. Mustapa, C.K. Cheng, Kinetic modeling and reaction pathways for thermo-catalytic conversion of carbon dioxide and methane to hydrogen-rich syngas over alpha-alumina supported cobalt catalyst, Int. J. Hydrogen Energy 46 (60) (2021) 30871–30881, https://doi.org/10.1016/j.ijhydene.2021.04.158.

[21] L. Fan, C.e. Li, L. van Biert, S.-H. Zhou, A.N. Tabish, A. Mokhov, P.V. Aravind, W. Cai, Advances on methane reforming in solid oxide fuel cells, Renew. Sustain. Energy Rev. 166 (2022) 112646, https://doi.org/10.1016/j.rser.2022.112646.

[22] X. Du, Y. Cheng, Z. Liu, H. Yin, T. Wu, L. Huo, C. Shu, CO2 and CH4 adsorption on different rank coals: a thermodynamics study of surface potential, gibbs free energy change and entropy loss, Fuel 283 (2021) 118886, https://doi.org/10.1016/j.fuel.2020.118886.

[23] H.N. Tran, E.C. Lima, R.-S. Juang, J.-C. Bollinger, H.-P. Chao, Thermodynamic parameters of liquid–phase adsorption process calculated from different equilibrium constants related to adsorption isotherms: a comparison study,

J. Environ. Chem. Eng. 9 (6) (2021) 106674, https://doi.org/10.1016/j.jece.2021.106674.
[24] M. Dargahi, E. Konkov, S. Omanovic, Influence of surface charge/potential of a gold electrode on the adsorptive/desorptive behaviour of fibrinogen, Electrochim. Acta 174 (2015) 1009–1016, https://doi.org/10.1016/j.electacta.2015.06.065.
[25] T. Horita, T. Shimonosono, H. Kishimoto, K. Yamaji, M.E. Brito, Y. Hori, H. Yokokawa, Visualization of oxygen ionization and flows in solid oxide fuel cells, Electrochem. Solid State Lett. 13 (12) (2010) B135, https://doi.org/10.1149/1.3489109.
[26] J.M. Clary, D. Vigil-Fowler, Adsorption site screening on a PGM-free electrocatalyst: insights from grand canonical density functional theory, J. Phys. Chem. C 127 (33) (2023) 16405–16413, https://doi.org/10.1021/acs.jpcc.3c03498.
[27] N.J. Williams, I.D. Seymour, D. Fraggedakis, S.J. Skinner, Electric fields and charge separation for solid oxide fuel cell electrodes, Nano Lett. 22 (18) (2022) 7515–7521, https://doi.org/10.1021/acs.nanolett.2c02468.
[28] E.C. Lima, A.A. Gomes, H.N. Tran, Comparison of the nonlinear and linear forms of the van't hoff equation for calculation of adsorption thermodynamic parameters (ΔS° and ΔH°), J. Mol. Liq. 311 (2020) 113315, https://doi.org/10.1016/j.molliq.2020.113315.
[29] W.-Y. Wang, G.-C. Wang, The first-principles-based microkinetic simulation of the dry reforming of methane over Ru(0001), Catal. Sci. Technol. 11 (4) (2021) 1395–1406, https://doi.org/10.1039/D0CY01942A.
[30] M.A. Al-Ghouti, D.A. Da'ana, Guidelines for the use and interpretation of adsorption isotherm models: a review, J. Hazard Mater. 393 (2020) 122383, https://doi.org/10.1016/j.jhazmat.2020.122383.
[31] X. Song, L.a. Wang, X. Ma, Y. Zeng, Adsorption equilibrium and thermodynamics of CO2 and CH4 on carbon molecular sieves, Appl. Surf. Sci. 396 (2017) 870–878, https://doi.org/10.1016/j.apsusc.2016.11.050.
[32] Y. Liu, Is the free energy change of adsorption correctly calculated? J. Chem. Eng. Data 54 (7) (2009) 1981–1985, https://doi.org/10.1021/je800661q.
[33] V.J. Inglezakis, S.G. Poulopoulos, 2 - adsorption, ion exchange, and catalysis, in: V. J. Inglezakis, S.G. Poulopoulos (Eds.), Adsorption, Ion Exchange and Catalysis, Elsevier, Amsterdam, 2006, pp. 31–56, https://doi.org/10.1016/B978-044452783-7/50002-1.
[34] J. Mou, Y. Gao, J. Wang, J. Ma, H. Ren, Hydrogen evolution reaction activity related to the facet-dependent electrocatalytic performance of NiCoP from first principles, RSC Adv. 9 (21) (2019) 11755–11761, https://doi.org/10.1039/C9RA01560D.
[35] S. Duan, M. Gu, X. Du, X. Xian, Adsorption equilibrium of CO2 and CH4 and their mixture on sichuan basin shale, Energy Fuel. 30 (3) (2016) 2248–2256, https://doi.org/10.1021/acs.energyfuels.5b02088.
[36] A.L. Myers, Thermodynamics of adsorption in porous materials, AIChE J. 48 (1) (2002) 145–160, https://doi.org/10.1002/aic.690480115.
[37] F. Calle-Vallejo, M.T.M. Koper, First-principles computational electrochemistry: achievements and challenges, Electrochim. Acta 84 (2012) 3–11, https://doi.org/10.1016/j.electacta.2012.04.062.
[38] S. Saren, F. Miksik, S. Seo, T. Miyazaki, K. Thu, Evaluation and development of improved thermodynamic models for adsorbed phase properties in adsorption cycles, Int. J. Heat Mass Tran. 229 (2024) 125579, https://doi.org/10.1016/j.ijheatmasstransfer.2024.125579.
[39] M. Seabaugh, NextCell versus NextCell-HP: comparing performance data, in: N. company (Ed.), Nextcell Versus NextCell-HP: Comparing Performance Data, Fuel Cell Materials, a Nexceris Company, 404 ENTERPRISE DRIVE, vol 43035, LEWIS CENTER, OH, 2017, p. 2.
[40] F. Zhong, X. Zhao, H. Fang, Y. Luo, S. Wang, C. Chen, L. Jiang, Unveiling optimal activity and mechanism of in situ Ni reduction Pr2Ni1-xZnxO4 anode for ammonia solid oxide fuel cells, Appl. Catal. B Environ. Energy 360 (2025) 124522, https://doi.org/10.1016/j.apcatb.2024.124522.
[41] S.A. Saadabadi, A. Thallam Thattai, L. Fan, R.E.F. Lindeboom, H. Spanjers, P. V. Aravind, Solid oxide fuel cells fuelled with biogas: potential and constraints, Renew. Energy 134 (2019) 194–214, https://doi.org/10.1016/j.renene.2018.11.028.
[42] M.D. Donohue, G.L. Aranovich, Classification of gibbs adsorption isotherms, Adv. Colloid Interface Sci. 76–77 (1998) 137–152, https://doi.org/10.1016/S0001-8686(98)00044-X.
[43] X. Tang, N. Ripepi, K. Luxbacher, E. Pitcher, Adsorption models for methane in shales: review, comparison, and application, Energy Fuel. 31 (10) (2017) 10787–10801, https://doi.org/10.1021/acs.energyfuels.7b01948.
[44] S. Sircar, Gibbsian surface excess for gas AdsorptionRevisited, Ind. Eng. Chem. Res. 38 (10) (1999) 3670–3682, https://doi.org/10.1021/ie9900871.
[45] F. Friebel, A.A. Mensah, Aging aerosol in a well-mixed continuous-flow tank reactor: an introduction of the activation time distribution, Atmos. Meas. Tech. 12 (5) (2019) 2647–2663, https://doi.org/10.5194/amt-12-2647-2019.
[46] J. Richter, F. Rachow, J. Israel, N. Roth, E. Charlafti, V. Günther, J.I. Flege, F. Mauss, Reaction mechanism development for methane steam reforming on a Ni/Al2O3 catalyst, Catalysts 13 (5) (2023) 884.
[47] M. Singh, S. Paydar, A.K. Singh, R. Singhal, A. Singh, M. Singh, Recent advancement of solid oxide fuel cells towards semiconductor membrane fuel cells, Energy Mater. 4 (1) (2024) 400012.
[48] B. Kumuk, N.N. Atak, B. Dogan, S. Ozer, P. Demircioglu, I. Bogrekci, Numerical and thermodynamic analysis of the effect of operating temperature in methane-fueled SOFC, Energies (2024).
[49] E. Yeo, H. Shin, T. Kim, S. Kim, J.S. Kang, Electrochemically driven capacitive CO2 capture technologies, J. Environ. Chem. Eng. 13 (2) (2025) 116092, https://doi.org/10.1016/j.jece.2025.116092.
[50] A.K. Demin, V. Alderucci, I. Ielo, G.I. Fadeev, G. Maggio, N. Giordano, V. Antonucci, Thermodynamic analysis of methane fueled solid oxide fuel cell system, Int. J. Hydrogen Energy 17 (1992) 451–458, https://doi.org/10.1016/0360-3199(92)90188-3.
[51] T.I. Tsai, L. Troskialina, A. Majewski, R. Steinberger-Wilckens, Methane internal reforming in solid oxide fuel cells with anode off-gas recirculation, Int. J. Hydrogen Energy 41 (1) (2016) 553–561, https://doi.org/10.1016/j.ijhydene.2015.10.025.
[52] N.G.H. Goselink, B.J. Boersma, L. van Biert, Evaluating the Thermodynamic Performance of an Sofc and Pemfc Combined System, Available at: SSRN 5147356.
[53] M. Tommasi, S.N. Degerli, G. Ramis, I. Rossetti, Advancements in CO2 methanation: a comprehensive review of catalysis, reactor design and process optimization, Chem. Eng. Res. Des. 201 (2024) 457–482, https://doi.org/10.1016/j.cherd.2023.11.060.
[54] B. Agún, A. Abánades, Comprehensive review on dry reforming of methane: challenges and potential for greenhouse gas mitigation, Int. J. Hydrogen Energy 103 (2025) 395–414, https://doi.org/10.1016/j.ijhydene.2025.01.160.
[55] Z. Xu, E.D. Park, Recent advances in coke management for dry reforming of methane over Ni-Based catalysts, Catalysts (2024).